RESEARCH   **Open Access**

New solid phase extractor based on ionic liquid functionalized silica gel surface for selective separation and determination of lanthanum

Hadi M Marwani[1,2*] and Amjad E Alsafrani[1]

Abstract

Background: Direct determination of metal ions, in particular at ultra-trace concentration, cannot be easily achieved in complex systems by analytical techniques because of the lack of sensitivity and selectivity of these methods. Therefore, an efficient separation step is often required prior to the determination of metal ions for sensitive, accurate, and interference-free determination of metal ions. In accordance, a new solid phase extractor based on silica gel functionalized with ionic liquid (SG-N-PhenacylPyrNTf$_2$) was developed for a selective separation of La(III) prior to its determination by inductively coupled plasma-optical emission spectrometry.

Methods: Immobilization of the ionic liquid on activated silica gel surface was confirmed by both Fourier transform infrared spectroscopy and scanning electron microscope. The concentration of ionic liquid on the surface of activated silica gel was determined based on thermal desorption method. The uptake behavior of the new SG-N-PhenacylPyrNTf$_2$ adsorbent toward metal ions was studied under static conditions by batch mode. The supernatant concentrations of metal ions were directly determined after filtration by inductively coupled plasma-optical emission spectrometry.

Results: Fourier transform infrared spectroscopy and scanning electron microscopy results strongly confirmed the formation of SG-N-PhenacylPyrNTf$_2$ phase. Adsorption isotherm study revealed the preference of SG-N-PhenacylPyrNTf$_2$ over activated silica gel for a selective separation of La(III) prior to its determination by inductively coupled plasma-optical emission spectrometry. Adsorption isotherm data were well fit the Langmuir adsorption model with a maximum adsorption capacity of 165.39 mg g^{-1} for La(III), which was consistent with that (167.08 mg g^{-1}) experimentally obtained from adsorption isotherm study. Kinetic study demonstrated that the adsorption of La(III) on the SG-N-PhenacylPyrNTf$_2$ phase followed the pseudo second-order kinetic model.

Conclusions: Ultimately, the developed method can be applied and effectively utilized for the determination of La(III) in natural water samples with acceptable and reliable results.

Keywords: N-PhenacylPyrNTf$_2$; Silica gel surface; La(III); Adsorption; ICP-OES; Batch mode

Background

Rare earth metals (REMs) have been used in different fields, such as chemical engineering, metallurgy, nuclear energy, optical, magnetic, luminescence, and laser materials, high-temperature superconductors, secondary batteries, and catalysis (Maestro and Huguenin 1995; Gaikwad and Damodaran 1993). Lanthanum is one of the REMs and has received special interest due to its technological importance and increasing demands for advanced new materials. Present day applications of lanthanum, as a pure element or in association with other compounds, are in super alloys, catalysts, special ceramics, and organic synthesis (Palmieri et al. 2002). However, most of the environmental problems are usually caused by human activities and natural resources. In recent years, this phenomenon is remarkably extended with the population density and growth of technology. There are several contaminants in nature, such as contamination with heavy metals, radionuclides, and lanthanides (Maanan 2008; Awwad et al. 2010). All of these are toxic and harmful to the public health, even at low

* Correspondence: hmarwani@kau.edu.sa
[1]Department of Chemistry, Faculty of Science, King Abdulaziz University, P.O. Box 80203, Jeddah 21589, Saudi Arabia
[2]Center of Excellence for Advanced Materials Research (CEAMR), King Abdulaziz University, P.O. Box 80203, Jeddah 21589, Saudi Arabia

concentration level (Cui et al. 2007). Thus, the most convenient way to overcome these problems is to apply selective extraction techniques, particularly when they exist at ultra-trace concentration level in complex matrix (Zang et al. 2010).

Various extraction techniques were implemented for the quantitative determination of trace metal ions, including liquid-liquid extraction (Khajeh 2011; Farajzadeh et al. 2009), coprecipitation (Komjarova and Blust 2006; Soylak and Erdogan 2006; Saracoglu et al. 2006), ion exchange (Tao and Fang 1998), cloud point extraction (Manzoori et al. 2007; Safavi et al. 2004), and solid-phase extraction (Zhang et al. 2012; Marahel et al. 2011; Duran et al. 2007). Recently, solid-phase extraction (SPE) has been widely used as a separation tool for the speciation of metal ions in environmental samples and has received much attention because of its advantages, such as absence of emulsion, high enrichment factor, disposal cost due to low consumption of reagent, and more importantly environment-friendly (Aydin and Soylak 2007; Simpson 2000). Nevertheless, the main limitation of SPE is the lack of selectivity (Jal et al. 2004), which leads to high interference of the other existing species with the target metal ion. The choice of a proper adsorbent plays an important role in SPE because it can control the analytical parameters, such as selectivity, affinity, and capacity (Cai et al. 2003; Dean 1998). Hence, different surface modification methods have been applied to classical SPE adsorbents (such as silica (Shin and Choi 2009) and polymer (Qiao et al. 2012)) in order to increase the selectivity.

Room-temperature ionic liquids (RTILs) have several unique chemical and physical properties which make it useful for wide applications in organic chemistry, inorganic chemistry, electrochemistry, and analytical chemistry (Zhao 2006; Vidal et al. 2012). RTILs have good thermal stability, negligible vapor pressure, tunable viscosity and miscibility with water, high conductivity, and high heat capacity (Handy 2005; Koel 2009). In addition, extraction and separation techniques applying solid adsorbents modified with ionic liquids (ILs) have become very active fields in analytical chemistry (Anderson et al. 2006). ILs can be immobilized on the surface of solid supports for additional applications as solid phase extractors of metal ions from their matrices or aqueous solutions (Mahmoud and Al-Bishri 2011). They have been immobilized on multiwalled carbon nanotubes (Wang et al. 2008), nanosilica (Mahmoud 2011; Mahmoud and Al-Bishri 2011), and silica gel (Ayata et al. 2011; Liang and Peng 2010). Silica gel (SG) adsorbents, as an example of inorganic solid phases, afford several advantages over organic solid phases, such as high porosity and hydrophilicity and ease of surface modification (Ngeontae et al. 2009; Quang et al. 2012). However,

research studies were little in the abovementioned field of the applications of supported ionic liquid phases.

In accordance, a solid phase extractant (SG-N-PhenacylPyrNTf$_2$) was developed based on a hybrid combination of the hydrophobic character of newly synthesized ionic liquid with SG properties, without the need for partition treatment by chelating compounds. Both Fourier transform infrared (FT-IR) spectroscopy and scanning electron microscope (SEM) confirmed the formation of the resulted SG-N-PhenacylPyrNTf$_2$ adsorbent. The selectivity of SG-N-PhenacylPyrNTf$_2$ toward different metal ions, including Co(II), Fe(II), Fe(III), La(III), and Ni(II) was investigated. The uptake behavior of the new SG-N-PhenacylPyrNTf$_2$ adsorbent toward La(III) was evaluated under batch conditions. Adsorption isotherm data were well fit with the Langmuir adsorption model, strongly supporting that the adsorption process was mainly monolayer on a homogeneous adsorbent surface. Kinetic study also demonstrated that the adsorption of La(III) on the SG-N-PhenacylPyrNTf$_2$ phase obeyed the pseudo second-order kinetic model. The proposed method was ultimately applied to real water samples with satisfactory results.

Experimental details
Chemicals and reagents
All reagents used were of high purity and of analytical reagent grade, and doubly distilled deionized water was used throughout experiments. N-phenacylpyridinium bromide (N-PhenacylPyrBr), bis(trifluoromethane)sulfonimide lithium (LiNTf$_2$), ethyl alcohol (Et-OH), and diethyl ether were purchased from Sigma-Aldrich (Milwaukee, WI, USA). SG (SiO$_2$, particle size 10 to 20 nm) with purity of 99.5% was also obtained from Sigma-Aldrich. Lanthanum nitrate [La (NO$_3$)$_3$] and stock standard solutions of 1,000 mg L^{-1} of Co(II), Fe(II), Fe(III), and Ni(II) were purchased from Sigma-Aldrich.

Preparation of the new solid phase extractor
Preparation of N-PhenacylPyrNTf$_2$ ionic liquid
N-PhenacylPyrNTf$_2$ ionic liquid was prepared according to previously reported standard method by Marwani (Marwani 2013; 2010). Specifically, an amount of 2 g N-PhenacylPyrBr was separately weighed and dissolved in 18.2 MΩ·cm distilled deionized water. The N-PhenacylPyrBr solution was then mixed with an equimolar amount of LiNTf$_2$. The resultant reaction mixture was stirred for 2 h at room temperature, and the reaction resulted in two phases. The lower layer was separated and dried under vacuum overnight.

Activation of SG
SG powder (25.0 g) was first activated by refluxing and stirring with 200 mL of 50% (*v*/*v*) concentrated

hydrochloric acid solution for 8 h in order to remove metal oxide and nitrogenous impurity and to enhance the content of silanol groups on the SG surface. The activated SG powder was filtered, repeatedly washed with 18.2 MΩ·cm distilled deionized water until acid-free and oven dried at 120°C for 5 h to remove surface-adsorbed water.

Synthesis of SG-N-PhenacylPyrNTf$_2$

The preparation of SG-N-PhenacylPyrNTf$_2$ was based on the immobilization of ionic liquid (N-PhenacylPyrNTf$_2$) on the surface of activated SG by a hybridization process of the hydrophobic character of ionic liquid with SG properties. An amount of 5 g activated SG was suspended in 100 mL ethyl alcohol, and 1 g N-PhenacylPyrNTf$_2$ was weighed, completely dissolved by warming in 50 mL ethyl alcohol and added to the activated SG suspension. The reaction mixture was stirred at 60°C for 12 h. The newly modified SG-N-PhenacylPyrNTf$_2$ phase was filtered and washed with 50 mL ethyl alcohol on three portions followed by doubly distilled deionized water and diethyl ether. The SG-N-PhenacylPyrNTf$_2$ adsorbent was then allowed to dry in an oven at 80°C for 5 h and kept in a desiccator for further use. The synthetic route of SG-N-PhenacylPyrNTf$_2$ is shown in Scheme 1.

Batch procedure

In this study, the effect of solution pH, adsorption capacity determination, effect of contact time, and effect of coexisting ions were investigated under static conditions by batch mode. For the effect of pH on the selectivity of SG-N-PhenacylPyrNTf$_2$ toward selected metal ions, standard solutions of 2 mg L^{-1} of each metal ion were prepared and adjusted to pH values ranging from 1.0 to 9.0, except for Fe(II) and Fe(III), with a series of buffer solutions, 0.2 mol L^{-1} HCl/KCl for pH 1.0 and 2.0, 0.1 mol L^{-1} CH$_3$COOH/CH$_3$COONa for pH 3.0 to 6.0, and 0.1 mol L^{-1} Na$_2$HPO$_4$/HCl for pH 7.0 to 9.0. Both Fe(II) and Fe(III) were prepared at the same concentration as above but were only studied with buffer solutions at pH values ranging from 1.0 to 4.0 in order to avoid any precipitation with buffer solutions at pH 5.0 to 9.0. Each standard solution was individually mixed with 20 mg of dry SG-N-PhenacylPyrNTf$_2$ phase. All mixtures were shaken vigorously at room temperature for 1 h to facilitate adsorption of the metal ions onto the SG-N-PhenacylPyrNTf$_2$. The supernatant concentration of metal ions was determined directly by inductively coupled plasma-optical emission spectrometry (ICP-OES) after filtration. For the study of La(III) adsorption capacity, standard solutions of 0, 5, 10, 20, 30, 40, 60, 80, 100, 125, 150, 200, and 500 mg L^{-1} were prepared as above, adjusted to the optimum pH value of 6.0 with the buffered aqueous solution (0.1 mol L^{-1} CH$_3$COOH/
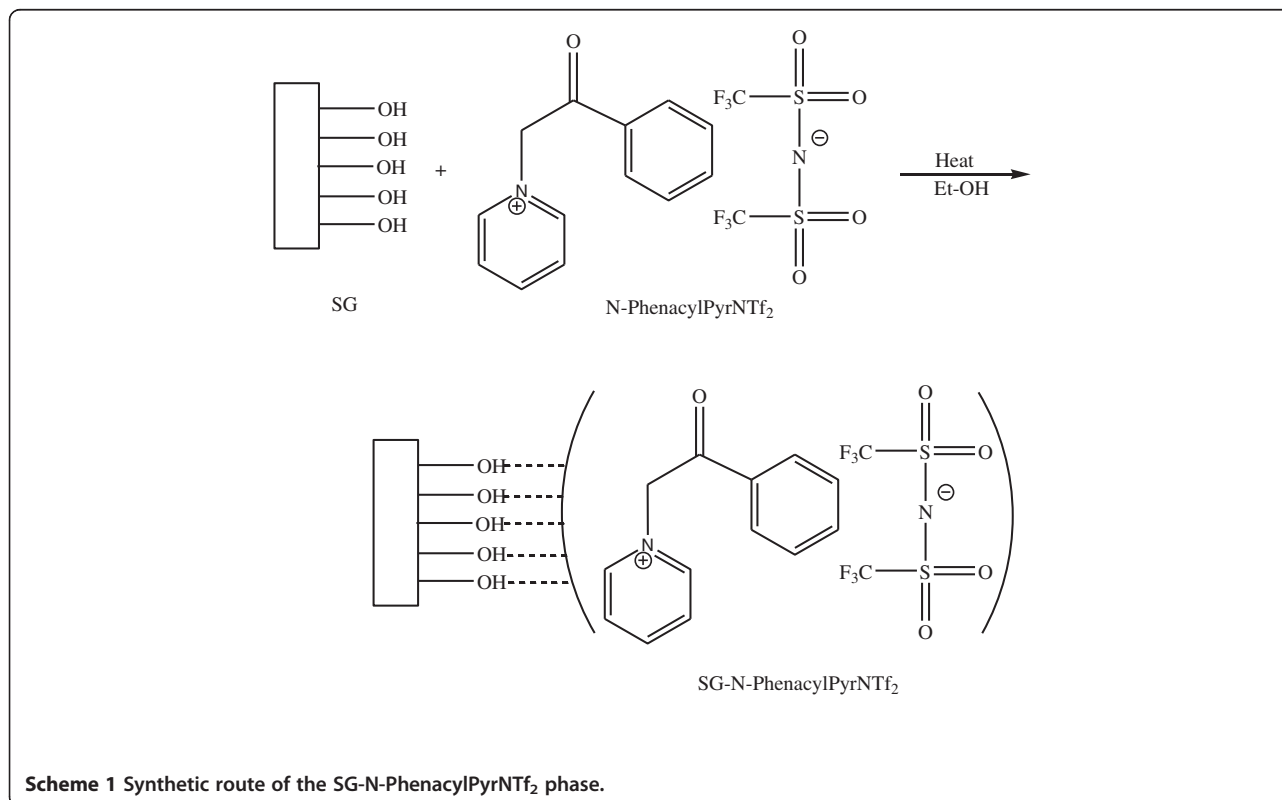
Scheme 1 Synthetic route of the SG-N-PhenacylPyrNTf$_2$ phase.

CH_3COONa) and individually mixed with 20 mg SG-N -PhenacylPyrNTf$_2$. The mixtures were mechanically shaken for 1 h at room temperature. In addition, the effect of shaking time on the La(III) uptake capacity was studied under the same batch conditions but at different equilibrium periods (2.5, 5, 10, 20, 30, 40, 50, and 60 min).

Methods

FT-IR spectra were recorded before and after modification of the SG phase on Perkin Elmer spectrum 100 series FT-IR spectrometer (Beaconsfield, Bucks, UK) in the range 4,000 to 600 cm^{-1}. A Jenway model 3505 laboratory pH meter (CamLab, Cambridgeshire, UK) was employed for the pH measurements and was calibrated with standard buffer solutions. Surface morphologies of SG before and after modification were investigated by SEM on a field emission scanning electron microscope (QUANT FEG 450, Amsterdam, Netherlands). The microscope was operated at an accelerating voltage of 15 kV. Thermolyne 47900 furnace was used to determine the millimoles per gram surface coverage value of SG-N-PhenacylPyrNTf$_2$ surface by thermal desorption analysis. ICP-OES measurements were acquired with the use of a Perkin Elmer ICP-OES model Optima 4100 DV, Shelton, CT, USA. The ICP-OES instrument was optimized daily before measurement and operated as recommended by the manufacturers. The ICP-OES spectrometer was used with the following parameters: FR power, 1,300 kW; frequency, 27.12 MHz; demountable quartz torch, Ar/Ar/Ar; plasma gas (Ar) flow, 15.0 L min^{-1}; auxiliary gas (Ar) flow, 0.2 L min^{-1}; nebulizer gas (Ar) flow, 0.8 L min^{-1}; nebulizer pressure, 2.4 bar; glass spray chamber according to Scott (Ryton), sample pump flow rate, 1.5 mL min^{-1}; integration time, 3 s; replicates, 3; and wavelength range of monochromator 165 to 460 nm. The wavelengths selected for the determination of Fe(II and III), Ni(II), Co(II), and La(III) were 238.204, 231.604, 228.616, and 348.902 nm, respectively.

Results and discussion

Determination of the surface coverage value of the SG-N-PhenacylPyrNTf$_2$ phase

An amount of 100 mg SG-N-PhenacylPyrNTf$_2$ adsorbent was weighed in a dry porcelain crucible. The weighed amount was then gradually heated into a furnace from 50°C to 700°C, and the ignited phase was kept at this temperature for 1 h. The remaining SG-N-PhenacylPyrNTf$_2$ phase was left to cool inside the furnace and then transferred to a desiccator. The weight loss of hydrophobic ionic liquid was determined by the difference in sample masses before and after the process of thermal desorption. Based on thermal desorption method, the concentration of N-PhenacylPyrNTf$_2$ was

determined to be 0.38 mmol g^{-1} on the surface of activated SG.

FT-IR and SEM characterization of SG-N-PhenacylPyrNTf$_2$

In order to emphasize the immobilization of the N-PhenacylPyrNTf$_2$ on activated SG surface, activated SG and SG-N-PhenacylPyrNTf$_2$ were evaluated by FT-IR spectroscopy. FT-IR spectrum of newly modified adsorbent shows spectral changes that are related to both N-PhenacylPyrNTf$_2$ and activated SG phases, confirming the formation of the new physically modified SG-N-PhenacylPyrNTf$_2$ phase. The band observed at 1,347 cm^{-1}, as displayed in Figure 1, was assigned to stretching vibrations of (NSO$_2$) bonds. Other characteristic bands of the SG-N-PhenacylPyrNTf$_2$ adsorbent appeared at the position of about 1,644 cm^{-1} for (C=C) and 1,713 cm^{-1} for (C=O). Two absorption peaks also appeared at 2,900 and 3,013 cm^{-1} which could be attributed to (–C–H) and (=C–H), respectively.

The formation of SG-N-PhenacylPyrNTf$_2$ phase was not only confirmed by FT-IR measurements but was also supported by taking SEM images of the activated silica gel and SG-N-PhenacylPyrNTf$_2$, as shown in Figure 2. Figure 2 displays a pronounced and characterized change of the surface morphology of activated SG as a result of the N-PhenacylPyrNTf$_2$ immobilization on the surface of activated SG. It can be clearly observed that the activated SG particles were collected in aggregate forms and completely covered with N-PhenacylPyrNTf$_2$. In addition, it is interesting to note that the particles of SG-N-PhenacylPyrNTf$_2$ (Figure 2B) are individually distributed in uniform and homogeneous shapes as compared to that of the activated SG (Figure 2A).
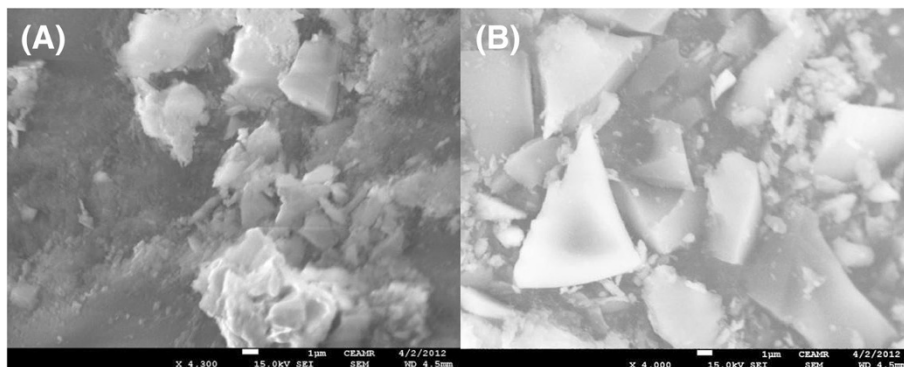

Figure 1 FT-IR of activated silica gel and SG-N-PhenacylPyrNTf$_2$ phases.
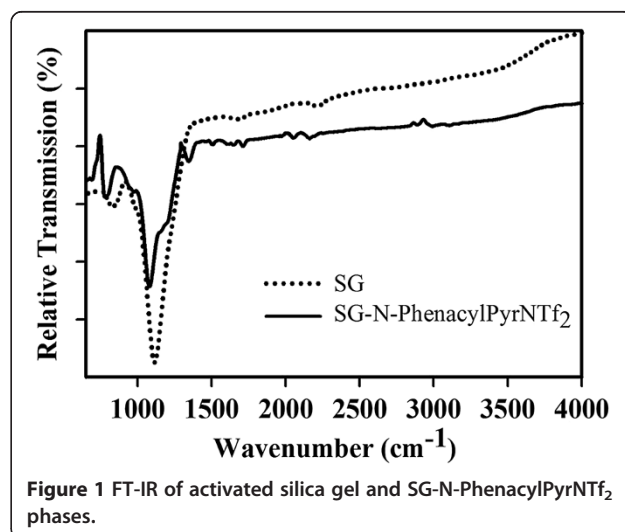
Figure 2 SEM images of (A) activated silica gel and (B) SG-N-PhenacylPyrNTf$_2$ phases.

Effect of pH and selectivity study

The acidity of solution plays an important role in the extraction of metal ions from different matrices. Therefore, the solution pH is the first parameter to be optimized. In order to evaluate the effect of pH on the adsorption of SG-N-PhenacylPyrNTf$_2$ toward Co(II), Fe(II), Fe(III), La(III), and Ni(II), pH values of the sample solution were studied in the range of 1.0 to 9.0 for all metal ions, except with Fe(II) and Fe(III) whose pH values were investigated in the range 1.0 to 4.0 in order to avoid any precipitation with buffer solutions at a pH value higher than 4.0. Selected metal ions of 2 mg L^{-1} were individually mixed with 20 mg SG-N-PhenacylPyrNTf$_2$ phase. All mixtures were mechanically shaken at room temperature for 1 h. Figure 3 depicts the effect of solution pH on the % extraction of selected metal ions. In general, it can be observed that there is an increase in % extraction of all metal ions with an increase in the pH. However, it is of interest to note that the highest % extraction is reached for La(III) among all metal ions included in this study. In addition, the selectivity of SG-N-PhenacylPyrNTf$_2$ phase toward La(III) was found to be the most among all metal ions at pH value of 6.0.

The distribution coefficient was calculated for each metal ion at its optimum pH value for further confirmation of the selectivity of SG-N-PhenacylPyrNTf$_2$ phase toward La(III), as illustrated in Table 1. The distribution coefficient (K_d) corresponding to the character of a metal ion adsorbed by an adsorbent (mL g^{-1}) can be obtained from the following equation (Han et al. 2005):

$$K_d = \frac{(C_i - C_e)}{C_e} \times \frac{V}{m} \quad (1)$$

where C_i and C_e correspond to initial and final concentrations (mg L^{-1}), respectively, V donates the volume of solution (mL), and m refers to the mass of adsorbent (g). Results presented in Table 1 clearly indicated that La(III) had the greatest K_d value up to 2.50×10^6 mL g^{-1} on the SG-N-PhenacylPyrNTf$_2$ adsorbent among all other metal ions even at their optimum pH values. These results strongly supported the finding that the selectivity of SG-N-PhenacylPyrNTf$_2$ was the most toward La(III).

The low % extraction of La(III) in the acidic medium could be ascribed to the presence of H$^+$ ion competing with the La(III) ion for the adsorption sites of SG-N-PhenacylPyrNTf$_2$ phase. At high pH values, the negative charge produced on the surface of activated SG and incorporated donor atoms (N, O, and S) presented in the N-PhenacylPyrNTf$_2$, as a result of the N-PhenacylPyrNTf$_2$
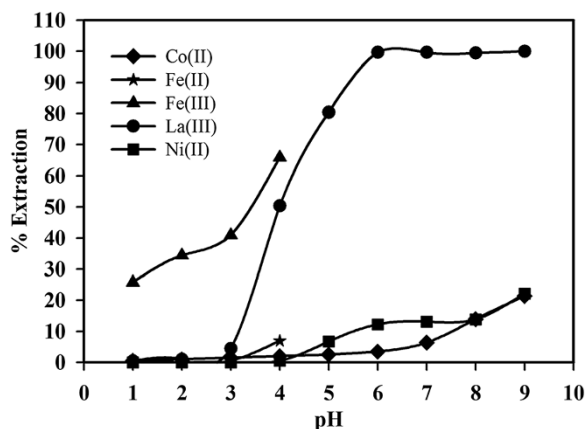

Figure 3 Effect of solution pH on the % extraction of selected metal ions.

Table 1 Selectivity study of 20 mg SG-N-PhenacylPyrNTf$_2$ toward different metal ions

Metal ion	Concentration (mg L^{-1})	q_e (mg g^{-1})	K_d (mL g^{-1})
Co(II)	2.00	0.54	340.33
Fe(II)	2.00	0.17	93.36
Fe(III)	2.00	1.65	2410.32
La(III)	2.00	2.50	2.50×10^6
Ni(II)	2.00	0.55	354.62

immobilization on the activated SG, strongly attained the selective adsorption of SG-N-PhenacylPyrNTf$_2$ toward La (III). Thus, the highest selectivity of the SG-N-PhenacylPyrNTf$_2$ phase toward La(III) may be attributed to electrostatic attraction or complex formation mechanism between SG-N-PhenacylPyrNTf$_2$ and La(III), as shown in Figure 4. Based on the above results, La(III) was selected among other metal ions for the study of other parameters controlling its maximum uptake on SG-N-PhenacylPyrNTf$_2$ under batch conditions and at the optimum pH value of 6.0.

Determination of La(III) adsorption capacity

To determine the loading capacity of SG-N-PhenacylPyrNTf$_2$, 25 mL aliquots of a series of La(III) concentrations (0 to 500 mg L^{-1}) were adjusted to pH 6.0, and the proposed separation procedure previously described above was applied. The amount of La(III) adsorbed at each concentration level was determined by ICP-OES. The adsorption profile of La(III) on 20 mg SG-N-PhenacylPyrNTf$_2$ was obtained by plotting the La(III)

concentration (mg L^{-1}) versus milligrams of La(III) adsorbed per gram SG-N-PhenacylPyrNTf$_2$ (Figure 5). From adsorption isotherm study, the adsorption capacity of SG-N-PhenacylPyrNTf$_2$ for La(III) was experimentally found to be 167.08 mg g^{-1}. The adsorption capacity of La(III) on the activated SG was also determined to be 85.06 mg g^{-1} under the same batch conditions as well as that of La(III) with SG-N-PhenacylPyrNTf$_2$ phase (Figure 5). These results indicated that the adsorption capacity for La(III) was increased by 96.43% with the newly modified SG-N-PhenacylPyrNTf$_2$ phase. The adsorption capacity of La(III) reported in the present study was also compared with those reported with SPE materials, as summarized in Table 2. As could be observed in Table 2, the adsorption capacity for La(III) obtained by SG-N-PhenacylPyrNTf$_2$ is comparable with those previously reported with other studies.

Adsorption isotherm models

In order to evaluate the adsorption of La(III) on SG-N-PhenacylPyrNTf$_2$ adsorbent, the adsorption isotherm model was evaluated using Langmuir and Freundlich isotherm models. The Freundlich isotherm model assumes that the adsorption occurs on heterogeneous surfaces. The Freundlich model is given by the following equation (Freundlich 1906):

$$\log q_e = \log K_f + 1/n \quad \log C_e \qquad (2)$$

where K_f and n are the Freundlich constants and can be calculated from the intercept and slope, respectively, of the linear plot of $\log q_e$ versus $\log C_e$.

The Langmuir isotherm model assumes that the adsorption occurs at specific homogeneous adsorption sites within the adsorbent and intermolecular forces that rapidly decrease with the distance from the adsorption surface
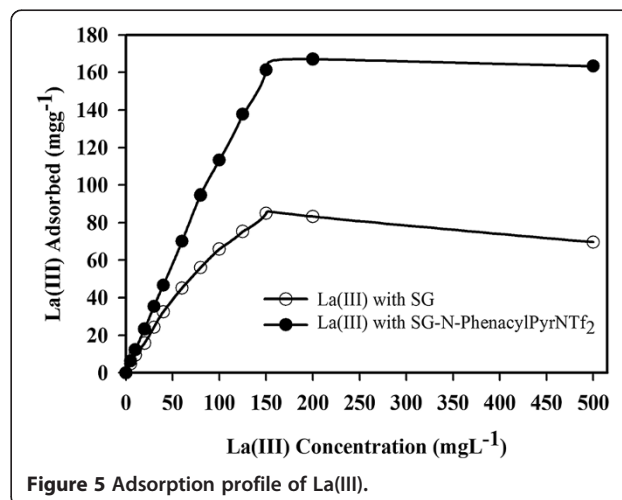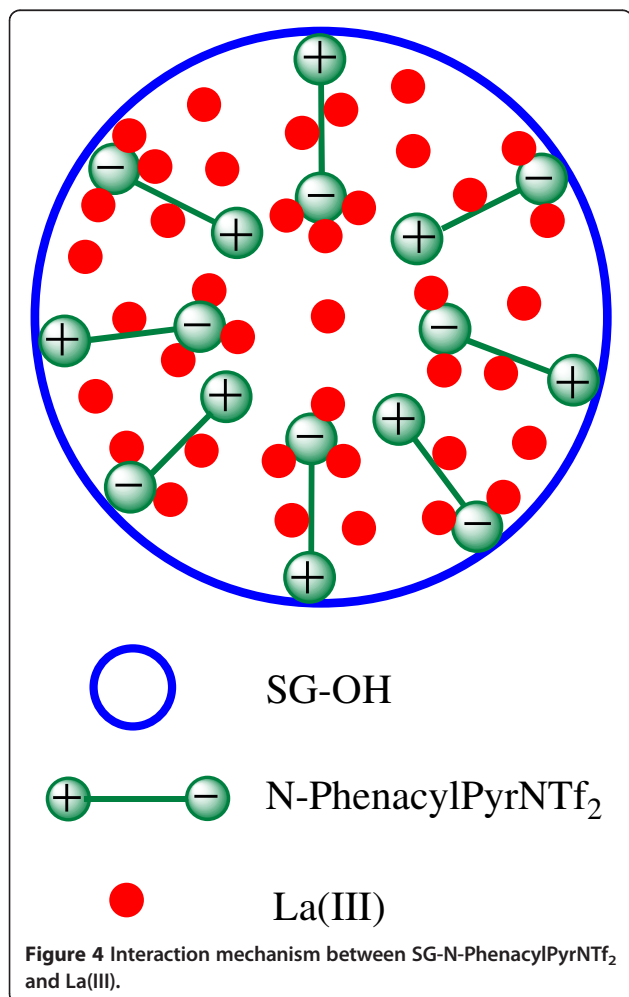

Figure 4 Interaction mechanism between SG-N-PhenacylPyrNTf$_2$ and La(III).

Figure 5 Adsorption profile of La(III).

Table 2 Comparison of SG-N-PhenacylPyrNTf$_2$ adsorption capacity for La(III) reported in the present study with other SPE materials

SPE material	Adsorption capacity (mg g^{-1})	Reference
SG-N-PhenacylPyrNTf$_2$	167.08	Present study
H,PEG400, PW[a]	220.80	(Zhang et al. 2009)
H,PEG400, PMo	214.40	(Zhang et al. 2009)
TA-MWCNTs[b]	5.35	(Tong et al. 2011)
MRH[c]	175.40	(Awwad et al. 2010)
Turbinaria conoides biomass	154.70	(Vijayaraghavan et al. 2010)
Powderized leaves of Platanus orientalis	28.65	(Sert et al. 2008)
MLTBC[d]	120.00	(Chen 2010)
XAD-4-OVSC[e]	2.30	(Jain et al. 2001)

[a]Polyethyleneglycol (PEG)-phosphomolybdic (PMo)/phosphotungstic (PW) heteropolyacids; [b]multiwalled carbon nanotube modified with tannic acid; [c]modified rice Husk activated carbon; [d]modified low-temperature bamboo charcoal; [e]amberlite XAD-4-o-vanillinsemicarbazone.

(Unlü and Ersoz 2006). The Langmuir model is described by the following equation (Langmuir 1916):

$$C_e/q_e = (C_e/Q_o) + 1/Q_o b \qquad (3)$$

where C_e corresponds to the equilibrium concentration of the metal ion in the supernatant (mg mL^{-1}) and q_e represents the amount of metal ion per gram of the adsorbent (mg g^{-1}). The symbols Q_o and b refer to Langmuir constants for SG-N-PhenacylPyrNTf$_2$ and are related to the maximum La(III) adsorption capacity (mg g^{-1}) and affinity parameter (L mg^{-1}), respectively. Langmuir constants can be obtained from a linear plot of C_e/q_e against C_e with a slope and intercept equal to $1/Q_o$ and $1/Q_o b$, respectively. In addition, the essential characteristics of the Langmuir adsorption isotherm can be represented in terms of a dimensionless constant separation factor or equilibrium parameter, R_L, which is defined as $R_L = 1/(1 + bC_o)$, where b is the Langmuir constant, indicating the nature of adsorption and the shape of the isotherm, and C_o is the initial concentration of the analyte of interest. The R_L value indicates the type of the isotherm, and R_L values lying between 0 and 1 indicates that the conditions were favorable for the adsorption process (McKay et al. 1982).

After evaluating both Freundlich and Langmuir isotherm models, it was found that adsorption isotherm data were well fit with the Langmuir model based on the least square fit. A close examination of Figure 6 reveals that a linear plot with correlation coefficient (R^2) value of 0.99 is obtained when plotting C_e/q_e against C_e. This result confirmed the validity of Langmuir adsorption isotherm model for the adsorption process of La(III) on SG-N-PhenacylPyrNTf$_2$. In consequence, adsorption

isotherm data indicated that the adsorption process was mainly monolayer on a homogeneous adsorbent surface.

The corresponding fitting parameters of Q_o and b of Langmuir isotherm model were also calculated and found to be 165.39 mg g^{-1} and 0.27 L mg^{-1}, respectively. The R_L value of La(III) adsorption on SG-N-PhenacylPyrNTf$_2$ was also determined to be 0.02, supporting a highly favorable adsorption process based on the Langmuir adsorption isotherm model. It is also of interest to notice that the La(III) adsorption capacity (165.39 mg g^{-1}) calculated from Langmuir equation was strongly consistent with that (167.08 mg g^{-1}) experimentally obtained from the adsorption isotherm study.

Effect of contact time

The influence of shaking time is an important factor for evaluating the affinity of SG-N-PhenacylPyrNTf$_2$ to La(III). The recommended static technique was carried out with a contact time varied from 2.5 to 60.0 min. Results of the effect of shaking time on the adsorption of La(III) on SG-N-PhenacylPyrNTf$_2$ phase provided that the SG-N-PhenacylPyrNTf$_2$ had rapid adsorption kinetics for La(III). As illustrated in Figure 7, over 152 mg g^{-1} La(III) was absorbed by the SG-N-PhenacylPyrNTf$_2$ phase after only 10 min of the equilibrium period. The loading capacity of La(III) was also raised up to more than 159 mg g^{-1} after 30 min until the maximum adsorption of SG-N-PhenacylPyrNTf$_2$ for La(III) was reached to 167.08 mg g^{-1} after 60 min.

Kinetic models

In order to analyze the uptake kinetic mechanism of La(III) adsorption on SG-N-PhenacylPyrNTf$_2$, several kinetic models were evaluated to find kinetic adsorption parameters correctly representing the nature of adsorption process. Conventionally, the kinetics of metal ion
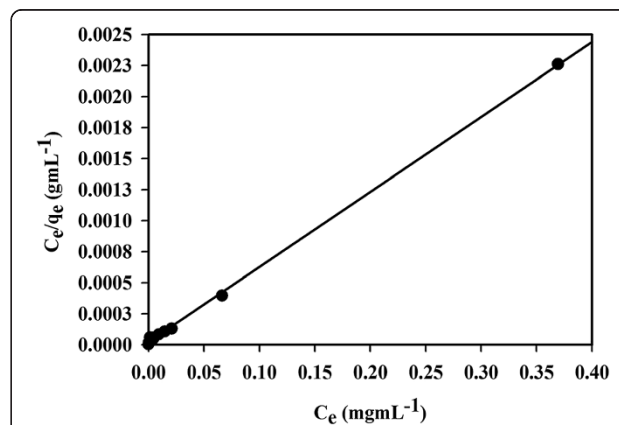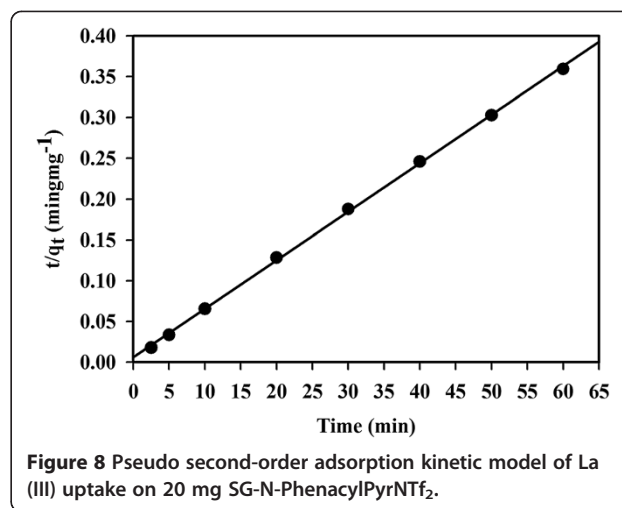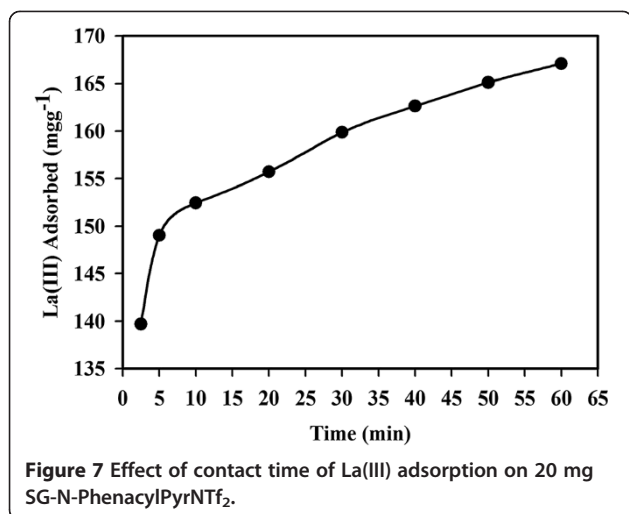

Figure 6 Langmuir adsorption isotherm model of La(III) adsorption on 20 mg SG-N-PhenacylPyrNTf$_2$ at pH 6.0 and 25°C.

Figure 7 Effect of contact time of La(III) adsorption on 20 mg SG-N-PhenacylPyrNTf$_2$.

Figure 8 Pseudo second-order adsorption kinetic model of La (III) uptake on 20 mg SG-N-PhenacylPyrNTf$_2$.

adsorption is described following the expressions originally given by Lagergren, known as the pseudo first-order adsorption, which are special cases for the general Langmuir rate equation (Wu et al. 2001). The pseudo first-order equation can be given by the following equation:

$$\log(q_e - q_t) = \log q_e - (k_1/2.303)t \tag{4}$$

where q_e (mg g^{-1}) and q_t (mg g^{-1}) are the amount of adsorption at equilibrium and at time t (min), respectively, and k_1 denotes the adsorption rate constant of pseudo first-order adsorption (min^{-1}). The adsorption rate constant k_1 and adsorption capacity q_e can be calculated from the slope and intercepts of the plot of $\log(q_e - q_t)$ against t.

In addition, the kinetics of La(III) adsorption on SG-N-PhenacylPyrNTf$_2$ was fit by the pseudo second-order kinetic model, which can be expressed as follows (Rao et al. 2009):

$$t/q_t = 1/v_o + (1/q_e)t \tag{5}$$

where $v_o = k_2\, q_e^2$ is the initial adsorption rate (mg g^{-1} min^{-1}) and k_2 (g mg^{-1} min^{-1}) corresponds to the rate constant of the pseudo second-order adsorption; q_e (mg g^{-1}) is the amount of metal ion adsorbed at equilibrium, and q_t (mg g^{-1}) refers to the amount of metal ion on the adsorbent surface at any time t (min). Kinetic parameters of q_e and v_o can be obtained from the slope and intercept, respectively, of the linear plots of t/q_t versus t.

Adsorption kinetics data were well fit by the pseudo second-order model (Figure 8). The correlation coefficient (R^2) factor was found to be 0.99, indicating that the pseudo second-order adsorption is more reliable and accurate. Kinetic parameters of q_e and v_o were found to be 168.18 mg g^{-1} and 167.40 mg g^{-1} min^{-1}, respectively, and k_2 was determined to be 0.01 g mg^{-1} min^{-1} of La(III) adsorption

on the SG-N-PhenacylPyrNTf$_2$ phase. The La(III) adsorption capacity on SG-N-PhenacylPyrNTf$_2$ obtained from the pseudo second-order kinetic model (168.18 mg g^{-1}) was also closely related to those obtained from adsorption isotherm experiments (167.08 mg g^{-1}) and from the Langmuir isotherm model (165.39 mg g^{-1}), supporting the highest applicability of the pseudo second-order nature of the La(III) adsorption by SG-N-PhenacylPyrNTf$_2$ and the validity of Langmuir adsorption isotherm model.

Performance of method in analytical applications
Effect of interfering ions
The effect of coexisting ions on the % extraction of La (III) was studied under optimized conditions in order to evaluate the applicability of proposed method for analytical applications in analyzing real samples. Model standard solutions containing fixed amount of 1 mg L^{-1} La (III) with either individual or mixed matrix ions were treated according to the recommended procedure. The tolerance limit of coexisting ions is defined as the largest amount making the recovery of analyte less than 90%. Results shown in Table 3 displayed that the extraction of La(III) was not affected by the medium composition containing either individual or mixed ions. This may be due to the low adsorption capacity or rate for interfering ions toward the SG-N-PhenacylPyrNTf$_2$ phase. Thus, it can be clearly concluded that the newly modified SG-N-PhenacylPyrNTf$_2$ phase has high selectivity toward La(III) when compared to other interfering ions, and the proposed method can be implemented for the determination of La (III) in real samples.

Application of the proposed method
In order to evaluate the applicability of the proposed procedure for the determination of targeted metal ion, the method was applied for the determination of La(III)

Table 3 Effect of matrix interferences on the extraction of 1 mg L^{-1} La(III) on 20 mg SG-N-PhenacylPyrNTf$_2$ ($N = 3$)

Coexisting ions	Concentration (mg L^{-1})	% Extraction of La(III)
Na^+, K^+, NH_4^+	7,000	97.13
Ca^{2+}, Mg^{2+}	7,000	98.07
Cd^{2+}	600	97.43
Co^{2+}	600	96.04
Fe^{2+}	600	95.57
Ni^{2+}	600	98.30
Pb^{2+}	600	96.36
Al^{3+}	300	98.25
Cr^{3+}	300	97.86
Cl^-, F^-, NO_3^-	4,000	98.39
CO_3^{2-}, SO_4^{2-}	3,000	97.77

in real water samples. For the analysis of water samples, four different water samples, including drinking, lake, sea, and tap water, were collected from Jeddah in Saudi Arabia. Water samples were analyzed using the standard addition method under the same batch conditions as above. Results displayed in Table 4 demonstrated that the % extraction of La(III) was in the range of 94.85% to 98.66%. Thus, the proposed method promoted the proportionality of SG-N-PhenacylPyrNTf$_2$ for the determination of La(III) in real water samples.

Conclusions

In this study, the immobilization of N-PhenacylPyrNTf$_2$ on activated SG, as a new solid phase extractor (SG-N-PhenacylPyrNTf$_2$), was successfully accomplished via electrostatic interaction. The SG-N-PhenacylPyrNTf$_2$ phase attained a perfect selectivity for the extraction

Table 4 Determination of La(III) at different concentrations in real water samples using 20 mg SG-N-PhenacylPyrNTf$_2$

Samples	Added (mg L^{-1})	Unadsorbed (mg L^{-1})	Extraction (%)
Tap water	1	0.02	98.00
	5	0.13	97.42
	10	0.39	96.15
Lake water	1	0.01	98.66
	5	0.14	97.22
	10	0.45	95.50
Seawater	1	0.03	97.40
	5	0.15	97.02
	10	0.52	94.85
Drinking water	1	0.02	98.46
	5	0.11	97.76
	10	0.36	96.45

and determination of La(III) in aqueous solution even in the presence of plentiful interfering ions. Results also demonstrated that adsorption isotherm data for La(III) adsorption on the SG-N-PhenacylPyrNTf$_2$ phase were well fit with the Langmuir classical adsorption isotherm model, providing that the formation of a monolayer over a homogeneous adsorbent surface. Moreover, kinetic isotherm data displayed that the adsorption of La(III) on the SG-N-PhenacylPyrNTf$_2$ phase obeyed a pseudo second-order kinetic reaction. Ultimately, the developed method can be applied and effectively utilized for the determination of La(III) in natural water samples with acceptable and reliable results.

References
Anderson JL, Armstrong DW, Wei G (2006) Ionic liquids in analytical chemistry. Anal Chem 78:2893–2902
Awwad NS, Gad HM, Ahmad MI, Aly HF (2010) Sorption of lanthanum and erbium from aqueous solution by activated carbon prepared from rice husk. Colloids Surf B 81:593–599
Ayata S, Bozkurt SS, Ocakoglu K (2011) Separation and preconcentration of Pb(II) using ionic liquid-modified silica and its determination by flame atomic absorption spectrometry. Talanta 84:212–215
Aydin FA, Soylak M (2007) A novel multi-element coprecipitation technique for separation and enrichment of metal ions in environmental samples. Talanta 73:134–141
Cai Y, Jiang G, Liu J, Zhou Q (2003) Multiwalled carbon nanotubes as a solid-phase extraction adsorbent for the determination of bisphenol A, 4-n-nonylphenol, and 4-tert-octylphenol. Anal Chem 75:2517–2521
Chen Q (2010) Study on the adsorption of lanthanum (III) from aqueous solution by bamboo charcoal. J Rare Earths 28:125–131
Cui Y, Chang X, Zhu X, Luo H, Hu Z, Zou X, He Q (2007) Chemically modified silica gel with p-dimethylaminobenzaldehyde for selective solid-phase extraction and preconcentration of Cr(III), Cu(II), Ni(II), Pb(II) and Zn(II) by ICP-OES. Microchem J 87:20–26
Dean JR (1998) Extraction methods for environmental analysis. Wiley, New York
Duran C, Gundogdu A, Bulut VN, Soylak M, Elci L, Sentürk HB, Tüfekci M (2007) Solid-phase extraction of Mn(II), Co(II), Ni(II), Cu(II), Cd(II) and Pb(II) ions from environmental samples by flame atomic absorption spectrometry (FAAS). J Hazard Mater 146:347–355
Farajzadeh MA, Bahram M, Zorita S, Mehr BG (2009) Optimization and application of homogeneous liquid-liquid extraction in preconcentration of copper (II) in a ternary solvent system. J Hazard Mater 161:1535–1543
Freundlich H (1906) Über die adsorption in lösungen (adsorption in solution). Z Phys Chem 57:384–470
Gaikwad AG, Damodaran AD (1993) Solvent extraction studies of holmium with acidic extractants. Sep Sci Technol 28:1019–1030
Han DM, Fang GZ, Yan XP (2005) Preparation and evaluation of a molecularly imprinted sol–gel material for on-line solid-phase extraction coupled with

high performance liquid chromatography for the determination of trace pentachlorophenol in water samples. J Chromatogr A 1100:131–136

Handy ST (2005) Room temperature ionic liquids: different classes and physical properties. Curr Org Chem 9:959–988

Jain VK, Handa A, Sait SS, Shrivastav P, Agrawal YK (2001) Pre-concentration, separation and trace determination of lanthanum(III), cerium(III), thorium(IV) and uranium(VI) on polymer supported o-vanillinsemicarbazone. Anal Chim Acta 429:237–246

Jal PK, Patel S, Mishra BK (2004) Chemical modification of silica surface by immobilization of functional groups for extractive concentration of metal ions. Talanta 62:1005–1028

Khajeh M (2011) Response surface modelling of lead pre-concentration from food samples by miniaturised homogenous liquid-liquid solvent extraction: Box-behnken design. Food Chem 129:1832–1838

Koel M (2009) Ionic liquids in chemical analysis. CRC Press, Boca Raton

Komjarova I, Blust R (2006) Comparison of liquid-liquid extraction, solid-phase extraction and co-precipitation preconcentration methods for the determination of cadmium, copper, nickel, lead and zinc in seawater. Anal Chim Acta 576:221–228

Langmuir I (1916) The constitution and fundamental properties of solids and liquids. J Am Chem Soc 38:2221–2295

Liang P, Peng L (2010) Ionic liquid-modified silica as sorbent for preconcentration of cadmium prior to its determination by flame atomic absorption spectrometry in water samples. Talanta 81:673–677

Maanan M (2008) Heavy metal concentrations in marine molluscs from the Moroccan coastal region. Environ Pollut 153:176–183

Maestro P, Huguenin D (1995) Industrial applications of rare earths: which way for the end of the century. J Alloys Compd 225:520–528

Mahmoud ME (2011) Surface loaded 1-methyl-3-ethylimidazolium bis (trifluoromethylsulfonyl)imide [EMIM$^+$Tf$_2$N] hydrophobic ionic liquid on nano-silica sorbents for removal of lead from water samples. Desalination 266:119–127

Mahmoud ME, Al-Bishri HM (2011) Supported hydrophobic ionic liquid on nano-silica for adsorption of lead. Chem Eng J 166:157–167

Manzoori JL, Abdolmohammad-Zadeh H, Amjadi M (2007) Ultra-trace determination of silver in water samples by electrothermal atomic absorption spectrometry after preconcentration with a ligand-less cloud point extraction methodology. J Hazard Mater 144:458–463

Marahel F, Ghaedi M, Montazerozohori M, Nejati Biyareh M, Nasiri Kokhdan S, Soylak M (2011) Solid-phase extraction and determination of trace amount of some metal ions on duolite XAD 761 modified with a new Schiff base as chelating agent in some food samples. Food Chem Toxicol 49:208–214

Marwani HM (2010) Spectroscopic evaluation of chiral and achiral fluorescent ionic liquids. Cent Eur J Chem 8:946–952

Marwani HM (2013) Exploring spectroscopic and physicochemical properties of new fluorescent ionic liquids. J Fluoresc 23:251–257

McKay G, Blair HS, Gardner JR (1982) Adsorption of dyes on chitin. I. Equilibrium studies. J Appl Polym Sci 27:3043–3057

Ngeontae W, Aeungmaitrepirom W, Tuntulani T, Imyim A (2009) Highly selective preconcentration of Cu(II) from seawater and water samples using amidoamidoxime silica. Talanta 78:1004–1010

Palmieri MC, Volesky B, Garcia O Jr (2002) Biosorption of lanthanum using sargassum fluitans in batch system. Hydrometallurgy 67:31–36

Qiao R, Zhang R, Zhu W, Gong P (2012) Lab simulation of profile modification and enhanced oil recovery with a quaternary ammonium cationic polymer. J Ind Eng Chem 18:111–115

Quang DV, Kim JK, Sarawade PB, Tuan DH, Kim HT (2012) Preparation of amino-functionalized silica for copper removal from an aqueous solution. J Ind Eng Chem 18:83–87

Rao MM, Kumar Reddy DHK, Venkateswarlu P, Seshaiah K (2009) Removal of mercury from aqueous solutions using activated carbon prepared from agricultural by-product/waste. J Environ Manage 90:634–643

Safavi A, Abdollahi H, Hormozi Nezhad MR, Kamali R (2004) Cloud point extraction, preconcentration and simultaneous spectrophotometric determination of nickel and cobalt in water samples. Spectrochim Acta Part A 60:2897–2901

Saracoglu S, Soylak M, Kacar Peker DS, Elci L, dos Santos WNL, Lemos VA, Ferreira SLC (2006) A pre-concentration procedure using coprecipitation for determination of lead and iron in several samples using flame atomic absorption spectrometry. Anal Chim Acta 575:133–137

Sert S, Kütahyali C, Inan S, Talip Z, Cetinkaya B, Eral M (2008) Biosorption of lanthanum and cerium from aqueous solutions by platanus orientalis leaf powder. Hydrometallurgy 90:13–18

Shin EM, Choi HS (2009) Column preconcentration and determination of cobalt (II) using silica gel loaded with 1-nitroso-2-naphthol. Bulletin of the Korean Chemical Society 30:1516–1520

Simpson NJK (2000) Solid phase extraction: principles, strategies and applications. Marcel Dekker, New York

Soylak M, Erdogan ND (2006) Copper(II)-rubeanic acid coprecipitation system for separation-preconcentration of trace metal ions in environmental samples for their flame atomic absorption spectrometric determinations. J Hazard Mater 137:1035–1041

Tao GH, Fang Z (1998) Dual stage preconcentration system for flame atomic absorption spectrometry using flow injection on-line ion-exchange followed by solvent extraction. J Anal Chem 360:156–160

Tong S, Zhao S, Zhou W, Li R, Jia Q (2011) Modification of multi-walled carbon nanotubes with tannic acid for the adsorption of La, Tb and Lu ions. Microchim Acta 174:257–264

Unlü N, Ersoz M (2006) Adsorption characteristics of heavy metal ions onto a low cost biopolymeric sorbent from aqueous solutions. J Hazard Mater 136:272–280

Vidal L, Riekkola M-L, Canals A (2012) Ionic liquid-modified materials for solid-phase extraction and separation: a review. Anal Chim Acta 715:19–41

Vijayaraghavan K, Sathishkumar M, Balasubramanian R (2010) Biosorption of lanthanum, cerium, europium, and ytterbium by a brown marine alga, turbinaria conoides. Ind Eng Chem Res 49:4405–4411

Wang Z, Zhang Q, Kuehner D, Xu X, Ivaska A, Niua L (2008) The synthesis of ionic-liquid-functionalized multiwalled carbon nanotubes decorated with highly dispersed Au nanoparticles and their use in oxygen reduction by electrocatalysis. Carbon 46:1687–1692

Wu F-C, Tseng R-L, Juang R-S (2001) Kinetic modeling of liquid-phase adsorption of reactive dyes and metal ions on chitosan. Water Res 35:613–618

Zang Z, Li Z, Zhang L, Li R, Hu Z, Chang X, Cui Y (2010) Chemically modified attapulgite with asparagine for selective solid-phase extraction and preconcentration of Fe(III) from environmental samples. Anal Chim Acta 663:213–217

Zhang L, Ding S-D, Yang T, Zheng G-C (2009) Adsorption behavior of rare earth elements using polyethyleneglycol (phosphomolybdate and tungstate) heteropolyacid sorbents in nitric solution. Hydrometallurgy 99:109–114

Zhang N, Peng H, Hu B (2012) Light-induced pH change and its application to solid phase extraction of trace heavy metals by high-magnetization Fe$_3$O$_4$@SiO$_2$@TiO$_2$ nanoparticles followed by inductively coupled plasma mass spectrometry detection. Talanta 94:278–283

Zhao H (2006) Innovative applications of ionic liquids as "green" engineering liquids. Chem Eng Commun 193:1660–1677